Eur J Pediatr (2009) 168:1449–1454
DOI 10.1007/s00431-009-0945-9

ORIGINAL PAPER

A novel *CLCN7* mutation resulting in a most severe form of autosomal recessive osteopetrosis

Nesrin Besbas · Markus Draaken · Michael Ludwig · Ozgur Deren · Diclehan Orhan · Yelda Bilginer · Fatih Ozaltin

Received: 17 January 2009 / Accepted: 9 February 2009 / Published online: 24 February 2009

Abstract Osteopetrosis is a bone disease characterized by osteoclast failure and impaired bone resorption. Genetically, it is classified in three forms with autosomal recessive (ARO), autosomal dominant, and intermediate autosomal recessive inheritance, respectively. Some ARO forms are also associated with primary neurodegeneration, retinal atrophy, and lysosomal storage, which are caused by *CLCN7* and *OSTM1* gene mutations. Herein, we present a unique consanguineous family with a 26-month-old child with osteopetrosis, neurodegeneration, retinal atrophy, and tubulopathy. Direct sequencing of the *CLCN7* gene showed a novel homozygous R561Q variant in the patient. Both healthy parents were heterozygous for this amino acid substitution indicating autosomal recessive inheritance. The same homozygous nucleotide transition was found prenatally in a second child and the pregnancy was terminated at 17th week of gestation. A full autopsy was performed to the fetus, which confirmed the presence of osteopetrosis, thereby indicating that the variant observed indeed represents the disease-causing mutation. This is the first report of ARO associated with a novel recessive R561Q variant in *CLCN7* gene, in which prenatal diagnosis was made.

Keywords Osteopetrosis · Autosomal recessive · *CLCN7* · Tubulopathy · Prenatal diagnosis

N. Besbas · Y. Bilginer · F. Ozaltin (✉)
Department of Pediatric Nephrology,
Hacettepe University Faculty of Medicine,
Sihhiye,
06100 Ankara, Turkey
e-mail: fozaltin@hacettepe.edu.tr

M. Draaken · M. Ludwig
Institut für Klinische Chemie und Pharmakologie,
Bonn, Germany

O. Deren
Department of Obstetrics and Gynecology,
Hacettepe University Faculty of Medicine,
Ankara, Turkey

D. Orhan
Department of Pediatric Pathology,
Hacettepe University Faculty of Medicine,
Ankara, Turkey

Introduction

Osteopetrosis is a genetic disorder characterized by osteoclast failure, thereby impaired bone resorption, which ranges widely in severity [17]. Since the disease is highly heterogeneous, clinical classification is difficult. Genetically, it is classified in three forms, namely autosomal recessive (ARO; *MIM 259700*), autosomal dominant (ADO; *MIM 166600*), and intermediate autosomal recessive (IARO; *MIM 259710*) inheritance, respectively [1, 4, 7]. The genes involved in human osteopetrosis are mostly associated with the control of intracellular and extracellular pH of osteoclasts. These include the genes encoding (1) the enzyme carbonic anhydrase type II (*CAII*), which catalyzes the hydration of CO_2 to H_2CO_3 [2]; (2) the alpha 3 subunit of the vacuolar H^+-ATPase of the ruffled border (*TCIRG1*) [6]; (3) the ruffled border Cl^- channel 7 (*CLCN7*) [9]; (4) the ostm1 protein (*OSTM1*) likely associated with the function of the Cl^- conductance [11, 12]; (5) plekhm1 protein (*PLEKHM1*) which is likely to be involved in vesicle trafficking and acidification [16]. Some autosomal recessive forms are known to be associated with primary neurodegeneration, retinal atrophy, and lysosomal storage (i.e., ceroid lipofuscinoses), which are caused by *CLCN7* or *OSTM1* gene mutations [8].

Herein, we present a unique consanguineous family with a child with osteopetrosis, neurodegeneration, retinal atrophy, and organomegaly probably associated with lysosomal storage, all of which are compatible with *CLCN7* mutation.

Patient and methods

Patient

A 26-month-old male patient was admitted to Hacettepe University Faculty of Medicine, Pediatric Nephrology Unit due to motor–mental retardation and blindness that were recognized when he was 3 months old. The parents were first degree relatives. In the physical examination, a significantly delayed motor and mental development was noted. The body weight and height were 11.400 g (between 10th and 25th percentile) and 86 cm (between 10th and 25th percentile), respectively. The head circumference was 52 cm (more than +2 SD). A gum hyperplasia, proptosis, and enlarged abdomen with marked hepatosplenomegaly were noted. In the neurological examination, axial hypotonicity and absence of bilateral pupil reactions were prominent. Ophtalmological examination showed disseminated pigmentary epithelial atrophy in the macula and the retina. He was not able to walk, sit, and talk. Laboratory evaluation of the patient was as follows: hemoglobin 10.9 g/dl, WBC 5,500/mm^3, platelet 300,000/mm^3, serum levels of alanine aminotransferase 167 IU/ml (*N* 5–40), aspartate aminotransferase 293 IU/ml (*N* 8–33), gamma glutamyl transpeptidase 94 IU/ml (*N* 5–40), glucose 111 mg/dl (*N* 70–110), blood urea nitrogen 9 mg/dl (*N* 5–18), creatinine 0.13 mg/dl (*N* 0.6–1.2), uric acid 1.83 mg/dl (*N* 2.7–8.5), calcium 9.5 mg/dl (*N* 8.6–10.2), phosphate 4 mg/dl (*N* 2.3–4.7) with normal 25-hydroxy vitamin D (27.3 μg/l, *N* 10–60) and increased intact parathyroid hormone levels (110 pg/ml, *N* 12–65), sodium 138 mEq/l (*N* 138–145), potassium 4.09 mEq/l (*N* 3.4–4.7), chloride 101 mEq/l (*N* 98–107), total protein 6.4 g/dl (*N* 6–8), and albumin 4.2 g/dl (*N* 3.8–5.4). In blood gas analysis, pH was 7.34 with a 23.7 mmol/l bicarbonate level. Urinalysis showed 30 mg/dl of proteinuria, with a specific gravity of 1,019, a pH of 7, and 500 mg/dl of glucosuria with normal sediment. Urinary beta-2 microglobulin was >20,000 ng/ml (*N* 0–300). Also, 24-h urinary calcium and protein excretion were 4.6 mg/kg (*N*<4 mg/kg/day) and 96 mg (*N*<150 mg/day), respectively. Tubular phosphate reabsorption was calculated as 85% with a 0.67 mmol/l of renal threshold for phosphate (TmP/GFR) (*N* 1.87±0.14 in neonates). Serology for toxoplasma, rubella, cytomegalovirus, herpes, and hepatitis virus was negative. Urine and serum amino acid analyses were normal. Tandem mass spectrophotometry showed no abnormality. Isoelectrofocussing of sialotransferrins on filter paper result was normal. Skeletal radiographs were compatible with osteopetrosis (Fig. 1). Abdominal ultrasonography detected a marked hepatosplenomegaly and increased echogenity in both kidneys. Cranial magnetic resonance imaging showed cerebral atrophy, ventricular dilatation, and bilaterally focal increased intensity in the occipital periventricular and subcortical white matter (gliosis). Electroencephalography and brain auditory-evoked potentials were normal. The patient never brought to visits for 2 years until the parents suddenly appeared seeking prenatal diagnosis for the second pregnancy at 15th week of the gestational age. At that time, we learned that the first sibling was suffering from pulmonary insufficiency in another hospital and died a few weeks later. Since we did not know the underlying genetic defect in the index case, we speeded up the genetic studies for the prenatal diagnosis of the second sibling. *CLCN7* gene was the first target to be screened due to typical clinical findings as well as consanguinity between parents suggesting autosomal recessive inheritance.

Mutational analysis

EDTA blood samples were obtained from patient and the parents. Isolation of genomic DNA was carried out by using the QIAmp DNA Blood Kit (Qiagen, Hilden, Germany). All 25 exons of *CLCN7* were amplified by standard PCR protocol. Primer sequences are available on request.

Fig. 1 Skeletal X-ray of the patient. Sclerotic bones along with multiple fracture lines that were typical for osteopetrosis were noted

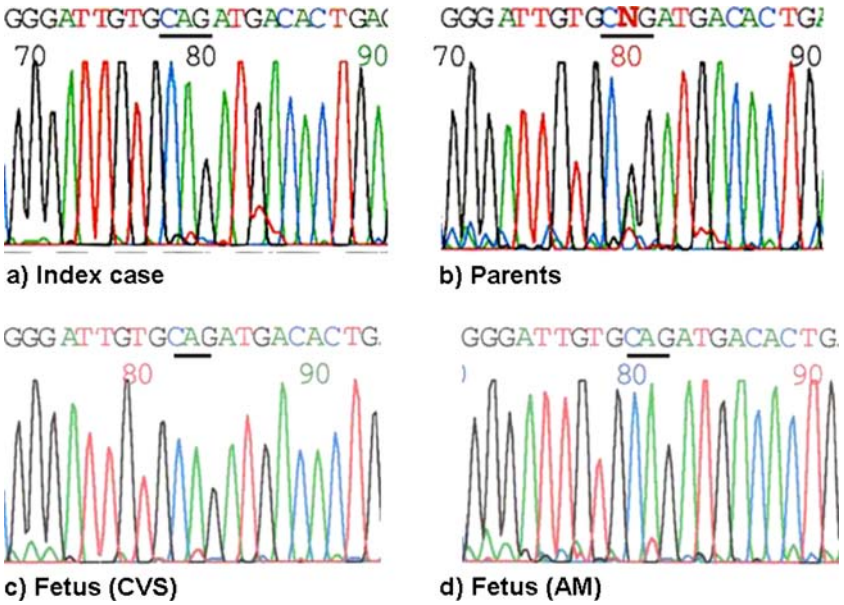

Fig. 2 Sequences of the exon 19 of the *CLCN7* in index case, the parents, and the fetus. Sequence analysis of the index case showed a homozygous adenine substitution for guanine at position c.1792, which resulted in a change of arginine at position 561 to glutamine (**a**); the parents were heterozygous for this variation (**b**); the fetus was also carrying this variation homozygously which was shown in both fetal samples (i.e., *CVS* chorion villus sampling (**c**) and *AM* amniocentesis (**d**))

Mutational analysis of *CLCN7* was performed by direct sequencing of all 25 exons of the gene including the flanking intronic regions. Variations observed were confirmed by sequencing the complementary strand. Segregation analysis was carried out in parental samples and DNA samples from 25 unrelated healthy Caucasians and 25 Turkish subjects (100 alleles) served as normal controls.

Restriction enzyme digestion

A restriction enzyme, HpyCH4H, that recognizes the mutant variant (TGCA instead of TGCG) was purchased and restriction digest was carried out according to the manufacturer's recommendations (New England Biolabs, Beverly, MA, USA). For this purpose, new primers were designed so that there would be a further recognition site in the PCR product that could serve as internal cutting control. Primers are available from the authors upon request.

Results

Mutational analyses

Direct sequencing of the *CLCN7* showed a homozygous adenine substitution for guanine at position c.1792 (GenBank acc. no. NM_001287) resulted in R561Q variant in exon 19 (Fig. 2). We also detected a heterozygous C/T variant in intron 20 (position −35). Segregation of R561Q was confirmed by direct sequencing of parental DNA samples, which were heterozygous for the same variation (Figs. 2 and 3). The absence of this variation was shown in 100 control chromosomes from healthy individuals of matched ethnic origin using restriction analysis. After the disease-causing mutation was defined in the index case, DNA was obtained from the fetus by both chorion villus sampling and amniocentesis at the 15th week of the gestational age. Forward and reverse sequences of the exon 19 of the *CLCN7* showed the same homozygous sequence in the fetus (Figs. 2 and 3) and the pregnancy was terminated at 17th week of gestational age.

Autopsy findings of the fetus

Postmortem radiologic examination revealed a uniform opacity of the skeletal tissue. Autopsy revealed hypertelorism and flattening of the nose. The costochondral

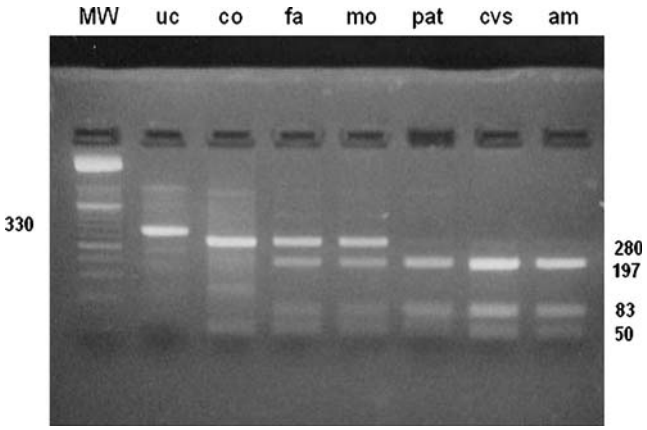

Fig. 3 Agarose gel electrophoresis using restriction enzyme. The uncut exon 19 PCR fragment has 330 bp; an internal recognition site (TGCA, cut by HpyCH4V) serves as control and produces fragments of 280 and 50 bp. If the mutation is present (TGCG mutated to TGCA), the 280-bp fragment is cut into two fragments of 197 and 83 bp. Products separated on a 4% agarose gel. *MW* weight marker (50-bp ladder); *uc* uncut control PCR fragment; *co* control; *fa* father; *mo* mother; *pat* patient; *cvs* chorion villus sampling; *am* amniocentesis sample

junctions were prominent. Histopathologic examination of the skeletal system showed normal cartilage, including the physeal growth zones. The osseous tissue formed by endochondral ossification exhibited persistence of calcified cartilage matrix, which was surrounded by excessive unremodeled primitive woven bone. There was no evidence of osteoclastic resorption of the bone. The intervening marrow spaces were markedly reduced in size (Figs. 4 and 5). Liver and spleen showed extramedullary hematopoiesis. None of the organs showed lysosomal storage findings.

Discussion

The first patient had a phenotype typical for autosomal recessive osteopetrosis (ARO) caused by *CLCN7* loss of function. Identification of this genetic defect in the index case has yielded prenatal diagnosis, which resulted in an early termination of the pregnancy and autopsy of the fetus that is the first in the literature.

CLCN7 analysis in the index patient revealed a novel homozygous R561Q variant that is also observed heterozygously in the first degree relative parents. This finding suggested that this missense variant is responsible for the phenotype observed. The question if the R561Q exchange is truly responsible for ARO in our patient or is only disease associated still remains to be elucidated in a functional assay. However, the absence of the G1792A transition in the SNP database and in 50 Caucasian and 50 Turkish control chromosomes argues against the possibility that this substitution is just a rare neutral variant. Also, autopsy findings in the fetus point towards a pathogenic role of this variant. In addition, several clues point to a critical role for arginine 561 in CLC-7 function: first, R561Q substitutes a polar residue for a basic one and, second, R561 is absolutely conserved at its corresponding position in CLC-7 and in other members of the family of chloride channels. These data and the apparent evolutionary conservation at least as far down as *Caenorhabditis elegans* suggest a critical role for this amino acid residue for proper CLC-7 function.

Osteopetrosis is a phenotype caused by several genetic abnormalities showing heterogeneous clinical manifestations. Mutations of several genes lead to impaired bone

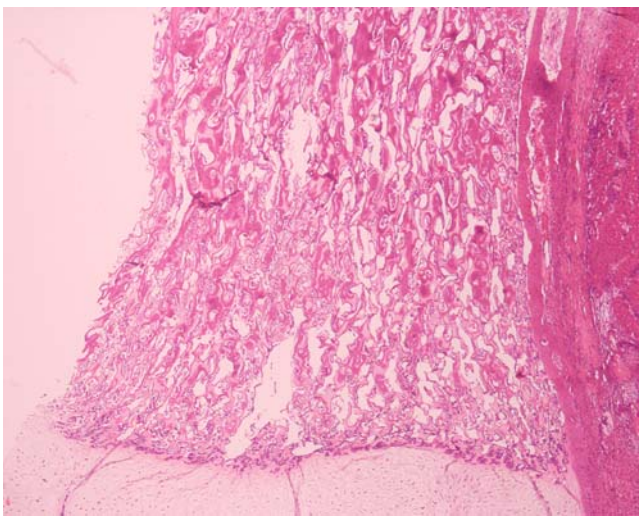

Fig. 4 Normal cartilage in the physeal growth zone and persistence of calcified cartilage (HE, original magnification ×20)

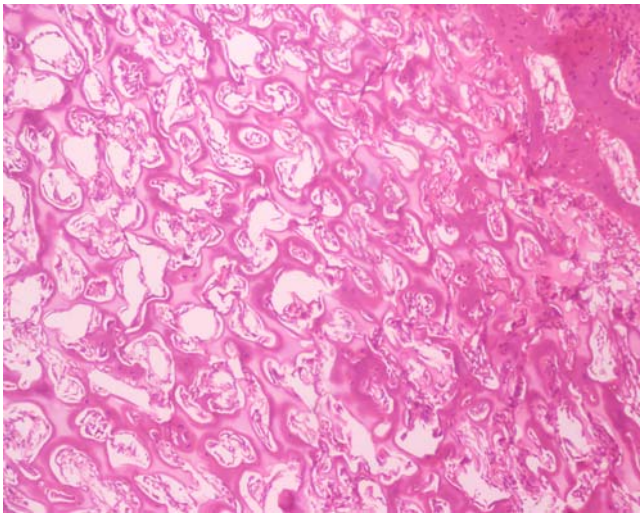

Fig. 5 Extremely dense and irregular bone trabecula, nearly all of which have a central core of cartilage (HE, original magnification ×100)

Table 1 Variants in *CLCN7* gene in the literature

Variant	Mode of inheritance	Reference
R561Q/R561Q	ARO	Our family
G203D/G203D	IARO	[3]
P470Q/P470Q	IARO	[3]
L766P/L766P	ARO	[5]
D145X/D145X	ARO	[7]
R767Q/R767Q	ARO	[7]
G240R/R526W	ARO	[7]
M332V/R767W	ARO	[7]
P249R/S744F	ARO	[7]
L614P/del-exon17	ARO	[7]
E374X/G306ins-54bp	ARO	[7]
Q555X/R762Q	ARO	[9]
I261F/I261F	ARO	[10]
delA*fs*X395/IVS21+1G→A	ARO	[14]

ARO autosomal recessive osteopetrosis, *IARO* intermediate autosomal recessive osteopetrosis

resorption and shared clinical features, which account for skeletal and hematological findings as well as the compression of the cranial nerves. Mutations in *CLCN7* have been previously identified in autosomal dominant osteopetrosis type II (ADO II), in some cases of ARO, and more recently in intermediate autosomal recessive osteopetrosis (IARO) (Table 1). Distinct mechanisms are likely to be responsible for these phenotypic variabilities with complete loss of function of the chloride channels in malignant ARO, some residual capacity in Cl^- conductance in intermediate osteopetrosis, and dominant negative effect in ADO II [3, 5, 6, 9]. The original ARO patient was compound heterozygote for a nonsense mutation (Q555X) in exon 18 and a missense mutation (R762Q) in exon 24, which are predicted to cause mRNA degradation and affect protein expression, respectively [9]. Our patient also had a severe motor–mental retardation and blindness as well as marked hepatosplenomegaly suggesting presence of a lysosomal storage disease. Lysosomal storage disease in the brain and retina in addition to osteopetrosis caused by *CLCN7* or *OSTM1* mutations has been reported [8, 11]. It is difficult to distinguish primary neurological changes related directly to the *CLCN7* gene defects and secondary effects caused by skull abnormalities affecting cerebral spinal fluid flow. However, both in animal models and in patients, histological, immunohistochemical, and ultrastructural studies provide evidence of a lysosomal storage, which is responsible for neurodegeneration including retinal atrophy [8, 11]. Visual impairment is frequently observed in patients with severe infantile osteopetrosis and has often been attributed to a compression of the optic nerve by the osteopetrotic process [15]. There are a few reports regarding central nervous system (CNS) degeneration in patients suffering from malignant infantile osteopetrosis [15]. Recently, Kasper et al. [8] have shown that *CLCN7* disruption leads to a widespread degeneration of the CNS with features of neuronal ceroid lipofuscinosis (NCL), a subtype of human lysosomal storage. An impairment of lysosomal function has been suggested as a common underlying mechanism. NCLs are genetically heterogeneous group of human progressive encephalopathies that are associated with neurocognitive and physical decline and ultimately lead to premature death [13]. This suggests that observed neurological abnormalities in several patients with osteopetrosis are caused by an NCL-like phenotype directly linked to *CLCN7* [7].

Interestingly, urinary findings of our patient characterized by glucosuria, phosphaturia, markedly elevated urinary beta-2 microglobulin, and tubular proteinuria clearly pointed to tubular dysfunction, which had never been described so far. This finding might be related to deposition of NCL storage material in proximal tubular cells, because it has been shown that this storage material in $Clcn7^{-/-}$ mice has been prominent in proximal tubular cells of KO but not WT kidneys [8]. However, since we did not demonstrate storage material deposition due to lack of autopsy, this remained speculative in our patient.

It is now possible to perform prenatal diagnosis by courtesy of huge efforts of various groups at least in affected families with known genetic alterations. Taking opportunity to identify the genetic defect in diseased sib, we were able to diagnose the second diseased child at 17th week of gestation, which has resulted in termination. The autopsy showed early typical histopathological changes of osteopetrosis, so the genetic diagnosis was confirmed. This is the first case that has been diagnosed during such an early period of life.

In conclusion, mutation in *CLCN7* gene should be looked for in autosomal recessive osteopetrosis. Since it is now possible to make the diagnosis of the disease prenatally, one should make every effort to avoid bearing multiple affected children.

References

1. Balemans W, Van Wesenbeeck L, Van Hul W (2005) Clinical and molecular overview of the human osteopetroses. Calcif Tissue Int 77:263–274
2. Bolt RJ, Wennink JM, Verbeke JI et al (2005) Carbonic anhydrase type II deficiency. Am J Kidney Dis 46:e71–e73
3. Campos-Xavier AB, Saraiva JM, Ribeiro LM et al (2003) Chloride channel 7 (CLCN7) gene mutations in intermediate autosomal recessive osteopetrosis. Hum Genet 112:186–189
4. Campos-Xavier AB, Casanova JL, Doumaz Y et al (2005) Intrafamilial phenotypic variability of osteopetrosis due to chloride channel 7 (CLCN7) mutations. Am J Med Genet A 133A:216–218
5. Cleiren E, Bénichou O, Van Hul E et al (2001) Albers–Schönberg disease (autosomal dominant osteopetrosis, type II) results from mutations in the ClCN7 chloride channel gene. Hum Mol Genet 10:2861–2867
6. Frattini A, Orchard PJ, Sobacchi C et al (2000) Defects in TCIRG1 subunit of the vacuolar proton pump are responsible for a subset of human autosomal recessive osteopetrosis. Nat Genet 25:343–346
7. Frattini A, Pangrazio A, Susani L et al (2003) Chloride channel ClCN7 mutations are responsible for severe recessive, dominant, and intermediate osteopetrosis. J Bone Miner Res 18:1740–1747
8. Kasper D, Planells-Cases R, Fuhrmann JC et al (2005) Loss of the chloride channel ClC-7 leads to lysosomal storage disease and neurodegeneration. EMBO J 24:1079–1091
9. Kornak U, Kasper D, Bösl MR et al (2001) Loss of the ClC-7 chloride channel leads to osteopetrosis in mice and man. Cell 104:205–215
10. Lam CW, Tong SF, Wong K et al (2007) DNA-based diagnosis of malignant osteopetrosis by whole-genome scan using a single-nucleotide polymorphism microarray: standardization of molecular investigations of genetic diseases due to consanguinity. J Hum Genet 52:98–101
11. Lange PF, Wartosch L, Jentsch TJ, Fuhrmann JC (2006) ClC-7 requires Ostm1 as a beta-subunit to support bone resorption and lysosomal function. Nature 440:220–223

12. Maranda B, Chabot G, Décarie JC et al (2008) Clinical and cellular manifestations of OSTM1-related infantile osteopetrosis. J Bone Miner Res 23:296–300
13. Mitchison HM, Lim MJ, Cooper JD (2004) Selectivity and types of cell death in the neuronal ceroid lipofuscinoses. Brain Pathol 14:86–96
14. Shin YJ (2004) Chloride channel CICN7 mutations in a Korean patient with infantile malignant osteopetrosis initially presenting with neonatal thrombocytopenia. J Perinatol 24:312–314
15. Steward CG (2003) Neurological aspects of osteopetrosis. Neuropathol Appl Neurobiol 29:87–97
16. Van Wesenbeeck L, Odgren PR, Coxon FP et al (2007) *PLEKHM1* is involved in osteoclastic vesicular transport and mutations in this gene cause osteopetrosis in *incisors absent* rat and human. J Clin Invest 117:919–930
17. Whyte MP (2002) Osteopetrosis. In: Royce PM, Steinman B (eds) Connective tissue and its heritable disorders: medical, genetic, and molecular aspects, 2nd edn. Wiley-Liss, New York, pp 753–770